IMPROVING ROCK BOLT DESIGN IN TUNNELS USING TOPOLOGY OPTIMISATION

Tin Nguyen[1], Kazem Ghabraie[2], Thanh Tran-Cong[3], Behzad Fatahi[4]

ABSTRACT

Finding an optimum reinforcement layout for underground excavation can result in a safer and more economical design, and therefore is highly desirable. Some works in the literature have applied topology optimisation in tunnel reinforcement design in which reinforced rock is modelled as homogenised isotropic material. Optimisation results, therefore, do not clearly show reinforcement distributions, leading to difficulties in explaining the final outcomes. In order to overcome this deficiency, a more sophisticated modelling technique in which reinforcements are explicitly modelled as truss elements embedded in rock mass media is employed. An optimisation algorithm extending the Solid Isotropic Material with Penalisation (SIMP) method is introduced to seek for an optimal bolt layout. To obtain the stiffest structure with a given amount of reinforced material, external work along the opening is selected as the objective function with a constraint on volume of reinforcement. The presented technique does not depend on material models used for rock and reinforcements and can be applied to any material model. Nonlinear material behaviour of rock and reinforcement is taken into account in this work. Through solving some typical examples, the proposed approach is proved to improve the conventional reinforcement design and provide clear and practical reinforcement layouts.

[1]PhD candidate, Computational Engineering and Science Research Centre, Faculty of Health, Engineering and Sciences, University of Southern Queensland, Toowoomba, QLD 4350, Australia. E-mail: tin.nguyen@usq.edu.au.

[2]PhD, Lecturer, School of Civil Engineering and Surveying, University of Southern Queensland, Toowoomba, QLD 4350, Australia. E-mail: kazem.ghabraie@usq.edu.au.

[3]PhD, Professor, Computational Engineering and Science Research Centre, University of Southern Queensland, Toowoomba, QLD 4350, Australia. E-mail: thanh.tran-cong@usq.edu.au.

[4]PhD, Senior lecturer, School of Civil and Environmental Engineering, University of Technology Sydney, Sydney, NSW 2007, Australia. E-mail: behzad.fatahi@uts.edu.au.

Keywords: tunnel reinforcement, rock bolt, topology optimisation, SIMP method.

INTRODUCTION

In tunnel reinforcement design with a wide range of rock mass types and complicated corresponding behaviour, selecting a design tool capable of considering complex rock mass conditions is important. With analytical approach, explicit calculations can be provided, however, its applicability is restricted to only simplified cases such as circular tunnels. Empirical methods which have been broadly used in the state-of-the-art reinforcement design, on the other hand, generally determine the support design based on classification systems. In heterogeneous and poor ground conditions these approaches can provide improper designs (Palmstrom and Stille 2007). Additionally, as constructed from long-term accumulated experiences in older projects, it is not guaranteed that the suggested design is the most reasonable one in both economical and technical terms for a particular situation. It is also worth noting that both empirical methods and analytical calculations are limited to free-field (Chen et al. 1999) and incapable of coping with the designs covering interaction between a new tunnel and adjacent structures. Owing to the ability in modelling complex ground conditions with consideration of discontinuities or adjacent structures, usage of numerical simulation has recently become common in tunnel excavation design (Gioda and Swoboda 1999; Jing 2003; Bobet et al. 2009). An appropriate combination of a numerical analysis method and an optimisation technique would provide a promising tool for obtaining an optimal tunnel reinforcement design.

Topology optimisation has been continuously developed and extended to a wide range of engineering applications in the past two decades. However, there have been limited works on utilising these optimisation methods in geotechnical, and particularly in tunnelling engineering (Ghabraie 2009). Yin et al. (2000) initiated by applying the homogenisation method in tunnel reinforcement design in which every element in the design domain is assumed as a square cell made of original rock surrounded by reinforced rock. The external work along the tunnel wall has been minimised under a prescribed reinforcement volume. Yin and Yang

(2000a) conducted further research on optimising tunnel support in various layered geological structure conditions. The solid isotropic material with penalization (SIMP) method was employed to determine the optimum distribution of reinforcement density in the design domain. In addition, tunnel and side wall heaves caused by swelling or squeezing rock, were addressed by Yin and Yang (2000b). This issue was also tackled by Liu et al. (2008b) using a fixed-grid bidirectional evolutionary structural optimisation (FG BESO) method. With regards to the shape optimisation of underground excavations, Ren et al. (2005) and Ghabraie et al. (2008) demonstrated the ability of evolutionary structural optimisation (ESO) method in searching for the optimal shape based on stress distribution. A simultaneous optimisation of shape and reinforcement distribution of an underground excavation for elastic material was explored by Ghabraie et al. (2010) using bi-directional evolutionary structural optimisation (BESO) method. It should be emphasized that all the earlier works on reinforcement optimisation have been restricted to linear elastic analysis, which is mostly not an appropriate assumption for geomechanical materials. This limitation has been removed by Nguyen et al. (2014) where nonlinear material models were considered in optimising tunnel reinforcement distribution.

In the above-mentioned works, to model the areas of the rock mass reinforced by rock bolts, a homogenised isotropic material which is stronger and stiffer than the unreinforced rock mass material is used . This modelling technique may result in a considerable reduction in computational time compared to explicit modelling of rock bolts. However, a perfect bonding between the reinforced material and the surrounding rock needs to be assumed for such modelling (Bernaud et al. 2009). More importantly, such a model can not consider the anisotropic nature of the reinforced rock which is significantly stronger in bolt direction and weaker in normal directions. Additionally, results obtained by such an approach need to be further processed to yield a clear bolt distribution design (see for example section 7.4 in Nguyen et al. 2014). To handle these shortcomings, one should model the reinforcements explicitly using linear inclusions embedded in the rock mass. This approach may take more

time and efforts especially in topology optimisation, but a higher level of accuracy could be achieved.

The scope of this work is to combine an extended optimisation technique and numerical analysis to seek for an optimal rock bolt configuration. Rock bolts are explicitly modelled and nonlinear behaviour of rock and bolts are considered in order to achieve a more practical and effective bolt design. The remaining parts of this paper are organised as follows. The next section presents the modelling of underground excavation and reinforcement installation, followed by a sensitivity analysis of reinforcement elements. A typical example is presented to show the application and efficacy of the proposed approach. A systematic study of various *in situ* stress states, optimisation parameters and ground conditions is performed to investigate their effects on optimised bolt layouts and also to illustrate the usefulness of the proposed method.

MODELLING OF TUNNEL EXCAVATION AND REINFORCEMENT SYSTEM

For simplicity, the considered tunnel is assumed to be long and straight enough to satisfy plane strain assumption. The support system employed to reinforce the tunnel excavation is a combination of a 100 mm-thick shotcrete lining and rock bolts. The shotcrete elements are attached to deform together with the rock elements around the excavation boundary. Rock bolts can be generally classified into two categories, namely anchored bolts and fully grouted bolts. This study focuses on pre-tensioned anchored bolts. Due to their small cross-section area, the bending stiffness of rock bolts can be neglected and hence truss elements are used here to model pre-tensioned bolts (Coda 2001; Leite et al. 2003). Rock bolts are embedded in the rock mass by connecting two ends of the bolts to nodes of the rock elements.

Some studies have attempted to simulate rock bolt designs in three dimensions (3D) (Grasselli 2005; Liu et al. 2008a). The main advantage of a 3D model over a 2D one is that the former is capable of exactly simulating actual fracture geometry, locations of bolted system and sequences of tunnel advancement and reinforcement installation. However, a 3D modelling also requires expensive computational cost and time. When performing an

optimisation in particular, the excessive computational time required for a 3D analysis is a major drawback as several analyses are required in solving an optimisation problem.

As tunnel construction is practically conducted in three-dimensions, a volume of ground material is squeezed into the opening, creating deformation around the opening. A straightforward modelling of support system in two-dimensional numerical tool is incapable of taking into account this 3D effect. To realistically simulate tunnel support in a plane strain condition, one needs to adopt assumptions accounting for the volume loss and deformations of the excavation boundary occurred before any support is installed. The convergence-confinement method (Panet and Guenot 1982) is adopted by applying a fictitious pressure inside the tunnel area to represent the effects of gradual decrease of the radial resistance. In the examples presented here, a fictitious pressure of 70% of the initial stress is applied to simulate this effect.

Sequences of excavation process and reinforcement installation are modelled with three separate steps with the aid of ABAQUS6.11. The *in situ* stress is imposed in the first step. The weight of ground material is neglected while the *in situ* stress is imposed to the model by creating an initial stress field with the considered horizontal to vertical stress ratio. Along the outer boundaries, the tangential tractions and normal displacements are confined while the nodal displacements of the elements on the excavation boundary are restrained to simulate the pre-excavation situation. The bolts and the shotcrete lining elements are absent in this step. In the second step, 70% of the calculated nodal forces around the opening are reversely applied to the excavation boundary. Deformation due to squeezing of ground material into the tunnel before rock bolt installation is simulated in this step. The final step includes removing the nodal forces and simultaneously activating the shotcrete lining elements and the bolts which are pre-tensioned to 60% of their yield stress capacity. It should be noted that these modelling assumptions explained above are by no means imposed by the optimisation approach. The proposed optimisation approach can be used with any other model including even 3D models without any modification.

PROBLEM STATEMENT AND OPTIMISATION METHOD

The aim of the tunnel reinforcement design is to employ a minimum amount of reinforcements while tunnel deformation after activating the reinforcements needs to be limited. This objective can be reformulated as finding the minimum tunnel deformation under a prescribed reinforcement volume. In the proposed method below, the optimisation process minimises the external work along the tunnel wall which is a functional of the tunnel deformation under a constrained reinforcement volume. The final solution is thus an optimised rock bolt distribution for a certain amount of bolt volume resulting in a minimum external work. It can be shown that any solution to this problem is also a solution to finding a minimum reinforcement volume subject to a constrained external work. The optimisation problem can be stated as

$$\begin{aligned} \min\ W &= \int \mathbf{f} \cdot d\mathbf{u} = \lim_{n\to\infty} \left[\frac{1}{2} \sum_{i=1}^{n} (\mathbf{u}_i - \mathbf{u}_{i-1}) \cdot (\mathbf{f}_i + \mathbf{f}_{i-1}) \right] \\ \text{subject to:} \quad V_R &= \sum_{m=1}^{t} A_m L_m \end{aligned} \tag{1}$$

where W is the total external work, $\mathbf{f}$ the external force vector, $\mathbf{u}$ the displacement vector, n the number of iterations in solving the non-linear equilibrium equations, V_R the given volume of rock bolt, A_m the cross section of rock bolt m, L_m the length of rock bolt m, and t number of rock bolts.

The *ground structure* concept (Bendsøe and Sigmund 2003) is used here. A ground structure is generated with all the possibilities of rock bolts one wishes to consider in the assigned design domain. Within a given ground structure, the proposed approach seeks for an optimal layout of rock bolts. In tunnel reinforcement design, these rock bolts have one of their ends on the tunnel opening and another in the rock mass. Using the ground structure, length of each rock bolt is fixed while its cross section area is selected as a function of a design variable. A power-law interpolation scheme, which is commonly used to define intermediate material properties in the SIMP method (Bendsøe 1989) is expressed below and employed

to define the cross section area of each rock bolt.

$$A_m = A_{min} + x_m^p (A_{max} - A_{min}) \tag{2}$$

Here A_{min} and A_{max} are the lower and upper bound values of cross section area, respectively. p is the penalty factor, and $0 \leq x_m \leq 1$ the design variable of rock bolt m. Selection of A_{min} and A_{max} restricts the desired range of cross section areas in the optimisation outcomes. Choosing $A_{min} = 0$, one enables the optimisation engine to completely eliminate unnecessary bolts if required.

The penalty factor is used to penalise the intermediate values and consequently push the cross section areas of bolts to the two extremes of A_{min} and A_{max}. Without penalisation ($p = 1$), the cross section area varies continuously from the lower to the upper bound values. On the other hand, a penalty factor $p > 1$ tries to push the intermediate values to the lower and upper bounds. The effect of penalisation then reduces to limiting the variety of bolt areas per unit length, ultimately leading to a reduction in the number of bolt types and/or in the number of drillings. It should be noted that using a very large value of the penalty factor results in local minima or convergence problem (Stolpe and Svanberg 2001). Selection of the penalty factor can have a considerable effect on optimisation results. Therefore, it needs to be carefully considered to meet technical aspects as well as economical terms. Effects of penalty factor are studied in Section 7 via a simple example.

It should be noted that as a two dimensional model is considered here, the obtained optimisation outcomes are bolt cross section areas per unit length of the tunnel. When translating the designs back to three dimensions, based on available bolt diameters and the limitations of the drilling machine, one can work out the spacing between bolts in the third dimension to satisfy the required area per unit length.

The sensitivity analysis presented in the next section is employed to update the cross section area of each bolt in each iteration. Further details on updating schemes for these

design variables can be found in Sigmund (2001). The process of finite element analysis and updating design variable continues until no design variable experiences a change of more than 10^{-4} in two consecutive iterations. The flowchart of the proposed approach is depicted in Fig. 1.

SENSITIVITY ANALYSIS

The sensitivity of the objective function due to an infinitesimal change in variable x is

$$\frac{\partial W}{\partial x} = \lim_{n\to\infty}\left[\frac{1}{2}\sum_{i=1}^{n}(\mathbf{u}_i - \mathbf{u}_{i-1})\cdot\left(\frac{\partial \mathbf{f}_i}{\partial x} + \frac{\partial \mathbf{f}_{i-1}}{\partial x}\right) + \frac{1}{2}\sum_{i=1}^{n}\left(\frac{\partial \mathbf{u}_i}{\partial x} - \frac{\partial \mathbf{u}_{i-1}}{\partial x}\right)\cdot(\mathbf{f}_i + \mathbf{f}_{i-1})\right] \quad (3)$$

As the considered problem is a displacement-controlled analysis, in Eq. (3) the second sum vanishes. Equilibrium requires the residual force vector to be eliminated and is stated as

$$\mathbf{R} = \mathbf{f} - \mathbf{p} = 0 \quad (4)$$

where $\mathbf{p}$ is the internal force vector. Combining Eq. (3) and Eq. (4) results in

$$\frac{\partial W}{\partial x} = \lim_{n\to\infty}\frac{1}{2}\sum_{i=1}^{n}(\mathbf{u}_i - \mathbf{u}_{i-1})\cdot\left(\frac{\partial \mathbf{p}}{\partial x} + \frac{\partial \mathbf{p}_{i-1}}{\partial x}\right) \quad (5)$$

The internal force vector is carried by both the rock material and the bolts and can be expressed as

$$\mathbf{p} = \mathbf{p}_m^S + \mathbf{p}^R \quad (6)$$

where $\mathbf{p}_m^S$ and $\mathbf{p}^R$ are the internal force vectors of the rock bolt m and the rock, respectively. The internal force vector carried by the rock is expressed as

$$\mathbf{p}^R = \sum_{e=1}^{M}\int_e \mathbf{C}_e\mathbf{B}\sigma d\nu = \sum_{e=1}^{M}\int_e \mathbf{C}_e\mathbf{B}\mathbf{D}_e^R\varepsilon d\nu \quad (7)$$

where M is the total number of rock elements, $\mathbf{C_e}$ the matrix which transforms the local force vector of element e to the global force vector, $\mathbf{B}$ the strain-displacement matrix and

$\mathbf{D}_e^R$ the matrix defining the stress-strain relationship of the rock. As $\mathbf{C}_e$, $\mathbf{B}$ and $\mathbf{D}_e^R$ are independent of variable x, differentiating Eq. (6) leads to

$$\frac{\partial \mathbf{p}}{\partial x_m} = \frac{\partial \mathbf{p}_m^S}{\partial x_m} \tag{8}$$

Substituting Eq. (8) into Eq. (5) results in

$$\frac{\partial W}{\partial x_m} = \lim_{n\to\infty} \frac{1}{2} \sum_{i=1}^{n} (\mathbf{u}_i - \mathbf{u}_{i-1}) \cdot \left(\frac{\partial \mathbf{p}_{m_i}^S}{\partial x_m} + \frac{\partial \mathbf{p}_{m_{i-1}}^S}{\partial x_m} \right) \tag{9}$$

The internal force vector in a rock bolt can generally be calculated from

$$\mathbf{p}_m^S(x_m, \delta_m) = A_m(x_m)\sigma(\delta_m) \tag{10}$$

where δ_m is the elongation of the rock bolt m and $\sigma(\delta_m)$ is the stress in the rock bolt which is a function of this elongation only. From Eq. (10) and Eq. (2), differentiation of internal force vector yields

$$\begin{aligned} \frac{\partial \mathbf{p}_m^S}{\partial x_m} &= p x_m^{p-1}(A_{max} - A_{min}) g(\delta_m) \\ &= p x_m^{p-1}(\mathbf{p}_m^{S_{max}} - \mathbf{p}_m^{S_{min}}) \end{aligned} \tag{11}$$

Substituting Eq. (11) and Eq. (8) into Eq. (5) results in the following

$$\begin{aligned} \frac{\partial W}{\partial x_m} &= p x_m^{p-1} \lim_{n\to\infty} \frac{1}{2} \sum_{i=1}^{n} (\mathbf{u}_i - \mathbf{u}_{i-1}) \cdot \left(\mathbf{p}_{m_i}^{S_{max}} - \mathbf{p}_{m_i}^{S_{min}} + \mathbf{p}_{m_{i-1}}^{S_{max}} - \mathbf{p}_{m_{i-1}}^{S_{min}} \right) \\ &= p x_m^{p-1}(\Pi_m^{S_{max}} - \Pi_m^{S_{min}}) \end{aligned} \tag{12}$$

where $\Pi_m^{S_{max}}$ and $\Pi_m^{S_{min}}$ are the total strain energies of the bolt m when its cross section areas are A_{max} and A_{min}, respectively. Setting $A_{min} = 0$ the above equation simplifies further to

$$\frac{\partial W}{\partial x_m} = p x_m^{p-1} \Pi_m^{S_{max}} \tag{13}$$

From Eq. (11), it can be seen that the sensitivity of a truss element is a direct measure of its total strain energy and only depends on the considered element.

It is important to note that the sensitivity analysis outcomes can be applied to any material models of the rock mass and bolts as no assumptions on material behaviour have been made in the above derivation.

IMPROVING THE UNIFORM ROCK BOLT DISTRIBUTION

A simple rock bolt design example is considered to illustrate the applicability and effectiveness of the proposed approach. The geometry of the tunnel is a rectangle of size $w \times h = 10\,\mathrm{m} \times 5\,\mathrm{m}$ augmented at the top with a semi-circle of radius 5 m. In order to ensure that the boundary effect is negligible, the modelled domain is chosen as a square of side length $20w$ (i.e. 200 m). Owing to symmetry, only half of this domain is modelled in the finite element analysis as displayed in Fig. 2. For a better view of the reinforcement layout, only an area around the opening with the size of $15\,\mathrm{m} \times 30\,\mathrm{m}$ will be illustrated in other figures.

A typical rock bolt design practice commonly involves determining three parameters, namely, length, spacing and cross section area of bolts. The bolts are empirically distributed uniformly around the areas of the opening which need to be reinforced and normal to the opening. Generally, the selection of bolt length is based on the thickness of unstable strata to ensure that the bolts are long enough to be firmly anchored in a competent rock mass. In homogeneous rock media, however, bolt length is selected to generate a radial compression to the rock arch increasing load carrying capacity of the rock arch. For the investigation of bolts in a weak homogeneous rock, following the suggestion of Dejean and Raffoux (1976), length of rock bolts should be in the range of $\frac{w}{3}$ to $\frac{w}{2}$, where w is the width of the opening. A fixed length of approximately 5 m is chosen herein.

Fixing the rock bolt length and its orientation, a ground structure can be generated by assuming a value for rock bolt spacing. In this example, a ground structure is created with a bolt spacing of 1 m and is codenamed GS10 as displayed in Fig. 3. It is worth noting that

the considered ground structure reflects the empirical suggestions with even distribution of bolts (Bieniawski 1979; Grimstad and Barton 1993). Effects of ground structure densities on optimisation outcomes will be discussed in Section 8.

Nonlinear material models are used to predict responses of the rock mass, shotcrete and rock bolts. The rock mass is modelled by an elasto plastic Mohr-Coulomb model with a non-associated flow rule, having a yield function and flow potential expressed as (Menétrey and Willam 1995)

$$F = R_{mc}q - p\tan\phi - c = 0 \tag{14}$$

$$G = \sqrt{\left(\epsilon C|_0 \tan\psi\right)^2 + \left(R_{m\omega}q\right)^2} - p\tan\psi \tag{15}$$

where

$$R_{mc}(\Theta,\phi) = \frac{1}{\sqrt{3}\cos\phi}\sin\left(\Theta+\frac{\pi}{3}\right) + \frac{1}{3}\cos\left(\Theta+\frac{\pi}{3}\right)\tan\phi, \tag{16}$$

$$R_{mw}(\Theta,e) = \frac{4(1-e^2)\cos^2\Theta + (2e-1)^2}{2(1-e^2)\cos\Theta + (2e-1)\sqrt{4(1-e^2)\cos^2\Theta + 5e^2 - 4e}}R_{mc}(\frac{\pi}{3},\phi), \tag{17}$$

$$R_{mc}(\frac{\pi}{3},\phi) = \frac{3-\sin\phi}{6\cos\phi}, \tag{18}$$

ϕ, c and ψ are the friction angle, cohesion and dilation angle of the rock, respectively. Θ the deviatoric polar angle, p is the mean stress, q the Mises stress, ϵ the meridional eccentricity, e the deviatoric eccentricity, and $C|_0$ the initial cohesion yield stress. The shotcrete and rock bolts are assumed to be elastic perfectly-plastic. A non-associated flow rule Drucker-Prager model is used to govern the shotcrete behaviour with the yield function and the flow potential being defined as

$$F = t - p\tan\beta - d = 0 \tag{19}$$

$$G = t - p\tan\psi \tag{20}$$

where

$$t = \frac{1}{2}q\left[1 + \frac{1}{K} - \left(1 - \frac{1}{K}\right)\left(\frac{r}{q}\right)^3\right] \tag{21}$$

$$p = -\frac{1}{3}\text{trace}(\sigma) \tag{22}$$

$$q = \sqrt{\frac{3}{2}\mathbf{S} : \mathbf{S}} \tag{23}$$

K is the ratio of yield stress in triaxial tension to yield stress in triaxial compression, $\mathbf{S}$ is the deviatoric stress. β, ψ and d are the friction angle, dilation angle and cohesion of rock material, respectively (ABAQUS 2013). The material properties of the rock mass, shotcrete lining and the rock bolts are summarised in Table 1. Typical properties of a very poor quality rock mass are used here (Hoek and Brown 1997).

The lower bound value of cross section areas A_{min} is assigned to be zeros to allow complete elimination of unnecessary bolts and the upper bound value is $649 \times 10^{-6}\,\text{m}^2$ (corresponding to the bolt diameter of 29 mm). No penalisation ($p = 1$) is applied in this example. The bolt volume constraint is selected as $34381\,\text{mm}^2/\text{m}$ (see Fig. 3). In this example, an *in situ* stress condition with vertical component of $\sigma_1 = 5\,\text{MPa}$ and horizontal stress ratio of $k = 0.4$ is considered. The optimised results are depicted in Fig. 4.

Fig. 4a displays the optimised bolt layouts with numbers at the end of bolts representing their cross section areas per unit length of the tunnel (mm^2/m). Since the tunnel is considered in plane strain condition, the obtained cross section areas per unit length can be converted to practical and appropriate spacings and sizes of bolts in three dimensions as noted before. It is noted that the plotted line width for each bolt is proportional to its cross section area. In order to demonstrate plastic behaviour around the opening, plastic strain magnitudes defined as $\sqrt{\frac{2}{3}\varepsilon^{pl} : \varepsilon^{pl}}$ (where ε^{pl} is the plastic strain tensor) are shown by colour-filled contour lines with a colour-bar on its right to define particular magnitudes. The elastic areas are coloured grey. It can be seen in Fig. 4a that more bolts are placed at the tunnel ribs where the largest plastic strains are observed.

The initial external work of the model is 1.37 MJ. A decrease in the objective function is obtained before reaching the convergence at the external work of 1.28 MJ (Fig. 4b). Hence, 6% improvement of the objective function is achieved which demonstrates the advantage of the obtained result compared with the empirical design.

To illustrate and compare tunnel convergence under the initial uniform and the optimised bolt layouts, displacements around the opening are displayed in Fig. 5. It can be seen that the proposed bolt layout provides smaller displacements nearly everywhere around the cavity, particularly at the tunnel ribs where a considerable displacement reduction is obtained. In other words, the presented algorithm has redistributed the initially uniform bolt layout to a more effective one.

Further advantages of this approach will be pointed out via further examples by examining various *in situ* stress and ground conditions. These examples will also demonstrate how this approach can be used to provide us with a better understanding of rock bolt design.

EFFECTS OF IN SITU STRESS CONDITIONS ON ROCK BOLT DESIGN

An investigation on effects of various *in situ* stress conditions on optimisation outcomes is conducted by varying magnitudes of vertical stress ($\sigma_1 = 3,\ 4,\ 5\,\text{MPa}$) and horizontal stress ratio ($k = 0.4,\ 1,\ 2$). A circular tunnel with a radius of 5 m is considered. The initial guess design is shown in Fig. 6. Other modelling and optimisation parameters are similar to the example described in Section 5. Fig. 7 displays all the obtained bolt layouts and the corresponding objective function variations.

For the case of hydrostatic stress state ($k = 1$), as expected, bolts are mostly distributed evenly around the opening (Figs. 7b, 7e and 7h). For the case of $k = 0.4$, more bolts are observed in the horizontal direction. Finally, for the case of $k = 2$, bolts are distributed mostly in vertical direction (Figs. 7c, 7f and 7i). It can be clearly seen that bolts tend to be distributed more densely at regions with large plastic strains.

With regards to the objective function variations, a stable convergence is observed in all cases (Fig. 7j). As expected, for the hydrostatic stress conditions, the optimised layouts are

just slightly different from the initial design and small improvements of approximately 0.3% are obtained for the objective function. For the other stress states, higher improvements are achieved with the largest value of 4.8% observable for $\sigma_1 = 4\,\text{MPa}$ and $k = 0.4$. The magnitudes of initial and optimised objective function and their relevant improvements are tabulated in Table 2 for all cases of stress states depicted in Fig. 7

EFFECTS OF PENALISATION ON OPTIMISATION OUTCOMES

In order to clearly show the role of the penalty factor (p) on optimisation outcomes, the example presented in Section 6 with the stress condition of $\sigma_1 = 4\,\text{MPa}$ and $k = 0.4$ is reconsidered with different values of penalty factor. The obtained optimised bolt layouts and variations of objective function are presented in Fig. 8.

By increasing the value of p from 1 to 3, the ineffective bolts are gradually eliminated, leading to a decline in the number of bolts (number of drillings) (Figs. 8a and 8b). However, as the value of p continues to increase to 7, the bolt layouts remain unchanged (Figs. 8b, 8c and 8d). It is worth noting that with those p values, the objective function converges at almost the same magnitudes (converged values are shown below each figure in Fig. 8). As p reaches 8, a convergence problem occurs with fluctuation of objective function about the optimised value obtained with smaller penalty factors (Fig. 8f). As expected, this example shows that using penalisation might result in a reduction of bolt numbers. However, it is observed that convergence problems might occur with large values of p.

EFFECTS OF GROUND STRUCTURE DENSITY ON OPTIMISATION OUTCOMES

Along with the ground structure GS10 introduced in Section 5, two other ground structures with different densities are generated to investigate their effects on the optimisation outcomes. One is with the bolt spacing of 0.5 m (codenamed GS05) as shown in Fig. 9a and the other one with the spacing of 1.5 m (codenamed GS15) as shown in Fig. 9b.

The *in situ* stress condition of $\sigma_1 = 3\,\text{MPa}$ and $k = 0.4$ is investigated and the obtained outcomes are detailed in Fig. 10 and Table 3.

It can be seen that the optimised bolt layouts are almost qualitatively similar for different ground structure densities (Fig.10a, 10b and 10c) with more bolts observed at the tunnel floor and tunnel ribs. However, various bolt densities result in various levels of improvements in the objective function. As tabulated in Table 3, there is not much difference in the initial values of external work for the three ground structures. Nevertheless, the objective function improvements are considerably different. While 8.4% and 4.8% improvements in the objective function are achieved for the ground structures GS05 and GS10, respectively, only 2% improvement is obtained for GS15. This is expected as denser ground structures provide more freedom and more choices to the optimisation algorithm to chose from. Therefore, to obtain higher improvements, it is beneficial to use a denser ground structure. However, in practice choosing a very small bolt spacing might result in damage around bearing plates due to stress concentration and also introduce more drilling work.

EFFECTS OF ROCK MATERIAL ON OPTIMISED BOLT LAYOUT DESIGN

Rock mass is naturally discontinuous with fractures, cracks, bedding planes, etc. A thorough consideration of fractures is necessary to obtain a more accurate model and hence a more reliable tunnel reinforcement design. To demonstrate the efficacy of the proposed approach for different material models, here a heavily jointed rock mass with highly densed parallel joint surfaces in different orientations is considered. A jointed material model supported in Abaqus 6.11 library is employed to describe the jointed rock mass behaviour. The jointed material model involves two governing behaviours for the bulk material and the joint systems (ABAQUS 2013). Bulk material is governed by the Drucker-Prager model. Additionally, the jointed material model includes a failure surface due to sliding in joint system a, which is expressed as

$$f_a = \tau_a - p_a \tan \beta_a - d_a = 0 \tag{24}$$

where τ_a and p_a are respectively the shear and normal stress along the joint surface. β_a and d_a are the friction angle and cohesion for system a, respectively.

Replacing the homogeneous model by the above jointed material model, the tunnel geometry investigated in Section 5 is reconsidered here. Two models, one with a horizontal set of joints and one with a vertical set of joints, are explored. Properties of the bulk material and the joint systems are identified in Table 4.

Fig. 11 displays the optimised bolt layouts for the cases of horizontal joints and vertical joints. It can be seen that the introduction of joint systems has altered the plastic strain and optimised bolt distributions around the opening. For the horizontal joints (Fig. 11a), the bolts are only present at the tunnel crown and tunnel floor. On the other hand, for the case of vertical joints (Fig. 11b), the bolts are concentrated at the corner of the tunnel crown and the tunnel ribs, and at the tunnel floor. Objective function values and obtained improvements are demonstrated in Fig. 11c and Table 5.

EFFECTS OF BEDDING PLANE ON OPTIMISED BOLT LAYOUT

This section aims to explore the effects of a bedding plane presence on optimised bolt layouts. The tunnel investigated in Section 5 is considered with the existence of a bedding plane at 1.5 m above the tunnel crown. A surface-based contact supported by ABAQUS6.11 is employed to model the interactions of surfaces. The mechanical behaviour of the surface interaction is governed by the Coulomb friction model in which the coefficient of friction (μ) is defined as the ratio between a shear stress and a contact pressure. A hydrostatic stress condition with a vertical stress of 5 MPa and two friction angles (ϕ) of the bedding plane, 5° and 15°, are investigated. Fig. 12 displays the achieved optimised bolt layouts and Table 6 tabulates the related objective functions.

It can be generally seen that with both values of friction angle, more bolts are distributed at the top of the tunnel where the bedding planes are located than the other positions around the opening (Figs. 12b and 12d). Also, the bolt volume at the tunnel crown of the case of friction angle of $\phi = 5^\circ$ is more than that of the friction angle of $\phi = 15^\circ$. In order to display slippage along the bedding planes, relative tangential displacement (RTD) is illustrated for the initial and the optimised bolt layouts. Clearly, the concentration of more bolts at the

tunnel top areas has partly reduced slippage along the bedding planes; especially for the case of friction angle of $\phi = 5°$. Additionally, further improvements of the objective functions are obtained as displayed in Fig. 12e and summarised in Table 6. Consequently, it can be concluded that the effects of the bedding planes can be effectively captured by the proposed method.

DISCUSSIONS AND CONCLUSIONS

A new approach incorporating an optimisation technique with numerical analysis has been introduced to search for improved rock bolt designs and proved to be a potentially useful tool in tunnel reinforcement design. By explicitly modelling the rock bolts, the proposed approach is capable of providing clearer, more accurate, more effective and more practical reinforcement layouts compared to earlier works in this area.

The proposed optimisation algorithm is independent of material models and thus the complexity of the models adopted in this approach is only limited to the capabilities of the method used for analysis. Furthermore, as the sensitivities are directly calculable from displacements, any analysis method which can provide the values of displacements under different loadings can be easily adopted in this approach. Nonlinear behaviour of both reinforcement material and rock in homogeneous media and fractured rock mass have been considered in this paper and finite element method is used as the method of analysis.

It has been shown that this approach can be effectively used to study and improve our understanding of effects of different parameters on optimised bolt layouts. The examples demonstrated that the commonly-employed empirical method where a uniform distribution of bolts is used is not necessarily optimal and can be further improved by the proposed approach. In the considered examples, reductions of up to 8% have been reported in the value of external work which was selected as the objective function.

In this study, the effects of ground structure and penalisation factor are demonstrated through some examples. Also, the impacts of *in situ* stresses, rock material properties and geological features such as bedding planes on optimised solutions are studied via several

examples.

Finding an optimal rock bolt design is a complicated problem which obviously needs to be studied in a case-by-case basis. The incorporation of advanced numerical modelling in the optimisation algorithm enables the proposed method to consider many significant factors in tunnelling design. Various ground conditions including *in situ* stress conditions, complex geomaterial properties, different geological features, or effects of adjacent constructions, etc. can be taken into consideration. Using this approach, it is also possible to study the effects of other important tunnelling features on optimal reinforcement layouts such as tunnel shapes or construction sequences. Consequently, the proposed method is expected to be a powerful tool in reinforcement design.

The proposed optimisation algorithm determines various bolt sizes around the opening to satisfy the given objective function while the bolt pattern has not been taken into account. In order to obtain a more effective bolt design, all bolt parameters including size and pattern should be accounted for in the optimisation algorithm. The authors are currently working on this matter to propose a more rational and powerful bolt design approach.

To the extent of this study, only minimisation of external work (equivalent to maximisation of structural stiffness of the design) has been considered. Other objective functions such as floor or side wall heave are also widely employed in tunnel design. The proposed approach can be easily extended to incorporate these objective functions as well.

ACKNOWLEDGEMENT

This is a part of the PhD work of the first author sponsored by CESRC, USQ and FHES. This financial support is gratefully acknowledged. We would like to thank the reviewers for their helpful comments.

REFERENCES

ABAQUS (2013). *ABAQUS/Abaqus Analysis User's Manual. Hibbit, Karlsson and Sorenson Inc.*

Bendsøe, M. P. (1989). "Optimal shape design as a material distribution problem." *Structural Optimization*, 1, 193–202.

Bendsøe, M. P. and Sigmund, O. (2003). *Topology Optimization: Theory, Methods and Applications*. Springer, Berlin, Heidelberg.

Bernaud, D., Maghous, S., de Buhan, P., and Couto, E. (2009). "A numerical approach for design of bolt-supported tunnels regarded as homogenized structures." *Tunnelling and Underground Space Technology*, 24, 533–546.

Bieniawski, Z. T. (1979). "The geomechanics classification in rock engineering applications." *ISRM Proceedings of the Fourth International Congress for Rock Mechanics, Montreux, Switzerland*, Rotterdam, A.A. Balkerma, 41–48.

Bobet, A., Fakhimi, A., Johnson, S., Morris, J., Tonon, F., and Yeung, M. R. (2009). "Numerical models in discontinuous media: Review of advances for rock mechanics applications." *Journal of Geotechnical and Geoenvironmental Engineeringenvironmental Engineering*, 135(11), 1547–1561.

Chen, L. T., Poulos, H. G., and Loganathan, N. (1999). "Pile responses caused by tunneling." *Journal of Geotechnical and Geoenvironmental Engineering*, 125(3), 207–215.

Coda, H. (2001). "Dynamic and static non-linear analysis of reinforced media: a BEM/FEM coupling approach." *Computers and Structures*, 79, 2751–2765.

Dejean, M. and Raffoux, J. F. (1976). "Role of rock bolting and parameters in its selection." *Mining Drifts and Tunnels: Tunnelling'76, London, Institute of Mining and Metallurgy*, 321–327.

Ghabraie, K. (2009). "Exploring topology and shape optimization techniques in undergorund excavation." Ph.D. thesis, RMIT University, Australia.

Ghabraie, K., Xie, Y. M., and Huang, X. (2008). "Shape optimisation of underground excavation using ESO method." *Innovations in Structural Engineering and Construction: Proceedings of the 4th International Structural Engineering and Construction Conference*, Melbourne, Australia, London Taylor and Francis, 877–882 (26-28 September).

Ghabraie, K., Xie, Y. M., Huang, X., and Ren, G. (2010). "Shape and reinforcement optimisation of underground tunnels." *Journal of Computational Science and Technology*, 4(1), 51–63.

Gioda, G. and Swoboda, G. (1999). "Developments and applications of the numerical analysis of tunnels in continuous media." *International Journal for Numerical and Analytical Methods in Geomechanics*, 23, 1393–1405.

Grasselli, G. (2005). "3D Behaviour of bolted rock joints: experimental and numerical study." *International Journal of Rock Mechanics and Mining Sciences*, 42, 13–24.

Grimstad, E. and Barton, N. (1993). "Updating of the Q-system for NMT." *International Symposium on Sprayed Concrete. Fagerness, Proceedings*, 46–66.

Hoek, E. and Brown, E. T. (1997). "Practical estimates of rock mass strength." *International Journal of Rock Mechanics and Mining Sciences*, 34(8), 1165–1186.

Jing, L. (2003). "A review of techniques, advances and outstanding issues in numerical modelling for rock mechanics and rock engineering." *International Journal of Rock Mechanics and Mining Sciences*, 40, 283–353.

Leite, L., Coda, H., and Venturini, W. (2003). "Two-dimensional solids reinforced by thin bars using the boundary element method." *Engineering Analysis with Boundary Elements*, 27, 193–201.

Liu, H. Y., Small, J. C., and Carter, J. P. (2008a). "Full 3D modelling for effects of tunnelling on existing support systems in the Sydney region." *Tunnelling and Underground Space Technology*, 23, 399–420.

Liu, Y., Jin, F., Li, Q., and Zhou, S. (2008b). "A fix-grid bidirectional evolutionary structural optimization method and its applications in tunnelling engineering." *International Journal for Numerical Methods in Engineering*, 73, 1788–1810.

Menétrey, P. and Willam, K. J. (1995). "Triaxial failure criterion for concrete and its generalization." *ACI Structural Journal*, 92, 311–318.

Nguyen, T., Ghabraie, K., and Tran-Cong, T. (2014). "Applying bi-directional evolution-

ary structural optimisation method for tunnel reinforcement design considering nonlinear material behaviour." *Computers and Geotechnics*, 55, 57–66.

Palmstrom, A. and Stille, H. (2007). "Ground behaviour and rock engineering tools for underground excavations." *Tunnelling and Underground Space Technology*, 22, 363–376.

Panet, M. and Guenot, A. (1982). "Analysis of convergence behind the face of a tunnel." *Tunnelling'82*, IMM, London, 197–203.

Ren, G., Smith, J. V., Tang, J. W., and Xie, Y. M. (2005). "Undergorund excavation shape optimization using an evolutionary procedure." *Computers and Geotechnics*, 32, 122–132.

Sigmund, O. (2001). "A 99 line topology optimization code written in Matlab." *Structural and Multidisciplinary Optimization*, 21, 120–127.

Stolpe, M. and Svanberg, K. (2001). "On the trajectories of penalization methods for topology optimization." *Structural and Multidisciplinary Optimization*, 21, 128–139.

Yin, L. and Yang, W. (2000a). "Topology optimization for tunnel support in layered geological structures." *International Journal for Numerical Methods in Engineering*, 47, 1983–1996.

Yin, L. and Yang, W. (2000b). "Topology optimization to prevent tunnel heaves under different stress biaxialities." *International Journal for Numerical and Analytical Methods in Geomechanics*, 24, 783–792.

Yin, L., Yang, W., and Guo, T. (2000). "Tunnel reinforcement via topology optimization." *International Journal for Numerical and Analytical Methods in Geomechanics*, 24, 201–213.

List of Tables

TABLE 1

Material properties	Rock	Rockbolt	Shotcrete
Young modulus (GPa)	1.4	200	25
Poisson's ratio	0.3	0.3	0.2
Friction angle (°)	24	-	30
Dilation angle (°)	0	-	12
Cohesion (MPa)	0.3	-	3
Yield stress (MPa)	-	400	20

TABLE 2

In situ stress	Objective function		Improvement (%)
	Initial (J)	Optimised (J)	
$\sigma_1 = 3\,\text{MPa},\ k = 0.4$	135171	132563	1.9
$\sigma_1 = 3\,\text{MPa},\ k = 1$	191557	191302	0.1
$\sigma_1 = 3\,\text{MPa},\ k = 2$	907087	885019	2.4
$\sigma_1 = 4\,\text{MPa},\ k = 0.4$	297788	283463	4.8
$\sigma_1 = 4\,\text{MPa},\ k = 1$	422782	421350	0.3
$\sigma_1 = 4\,\text{MPa},\ k = 2$	2149557	2102266	2.2
$\sigma_1 = 5\,\text{MPa},\ k = 0.4$	467175	449962	3.6
$\sigma_1 = 5\,\text{MPa},\ k = 1$	830538	827360	0.4
$\sigma_1 = 5\,\text{MPa},\ k = 2$	4210250	4088152	2.9

TABLE 3

Ground structure	Objective function		Improvement (%)
	Initial (J)	Optimised (J)	
GS05	344021	314947	8.4
GS10	344098	327392	4.8
GS15	343410	336584	2

TABLE 4

Material properties	Bulk material	Joint surface
Young modulus (GPa)	5	-
Poisson's ratio	0.3	-
Friction angle (°)	35	26
Dilation angle (°)	5	12
Cohesion (kPa)	6×10^3	70

TABLE 5

Ground condition	Objective function		Improvement (%)
	Initial (J)	Optimised (J)	
Rock mass with horizontal joints	218925	216038	1.3
Rock mass with vertical joints	258340	255437	1.1

TABLE 6

Friction angle	Objective function		Improvement (%)
	Initial (J)	Optimised (J)	
$\phi = 5^\circ$	1400179	1355220	3.2
$\phi = 15^\circ$	1176049	1167870	0.6

List of Figures

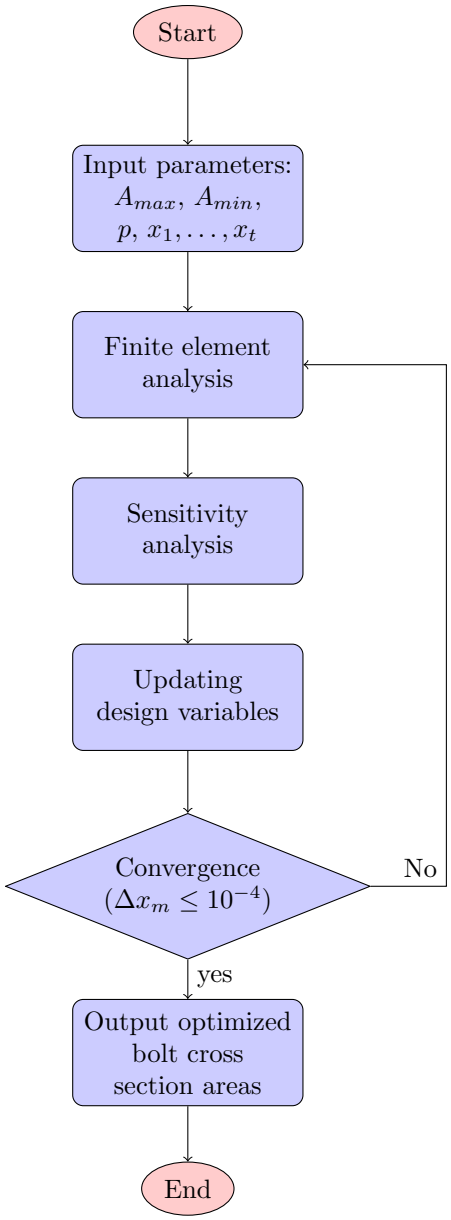
Start
Input parameters: A_{max}, A_{min}, p, $x_1, \ldots, x_t$
Finite element analysis
Sensitivity analysis
Updating design variables
Convergence ($\Delta x_m \leq 10^{-4}$)
No
yes
Output optimized bolt cross section areas
End

FIG. 1

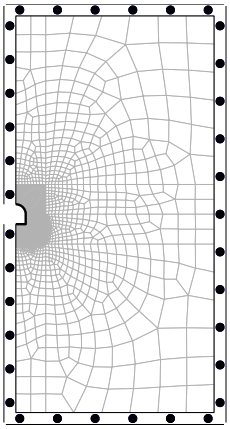

FIG. 2

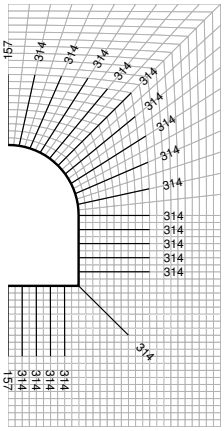
157
314
314
314
314
314
314
314
314
314
314
314
314
314
314
314
157

FIG. 3

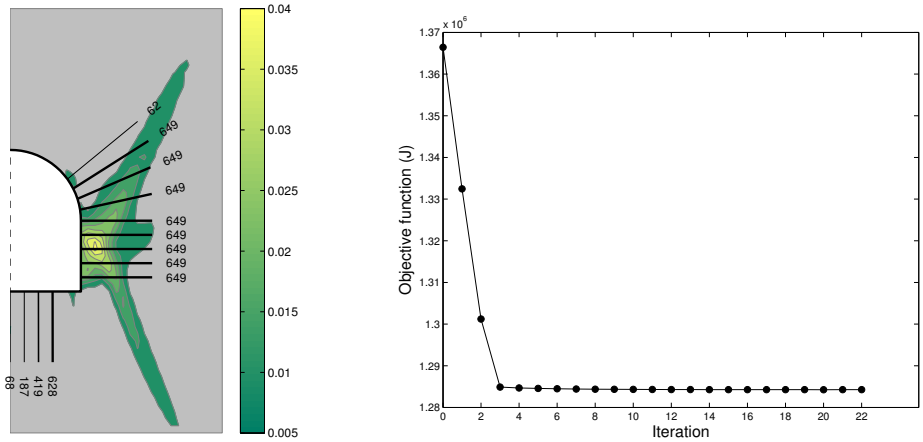
0.04
0.035
0.03
0.025
0.02
0.015
0.01
0.005
62
649
649
649
649
649
649
649
649
68
187
419
628
x 10^6
1.37
1.36
1.35
1.34
1.33
1.32
1.31
1.3
1.29
1.28
Objective function (J)
0
2
4
6
8
10
12
14
16
18
20
22
Iteration

(a) (b)

(a) (b)

FIG. 4

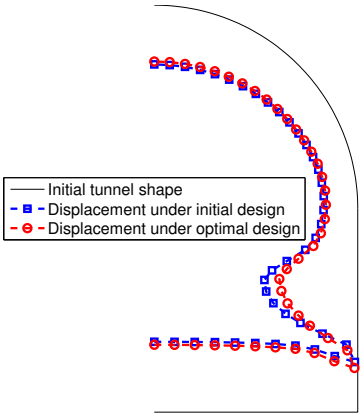
Initial tunnel shape
Displacement under initial design
Displacement under optimal design

FIG. 5

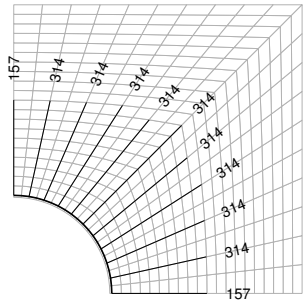

FIG. 6

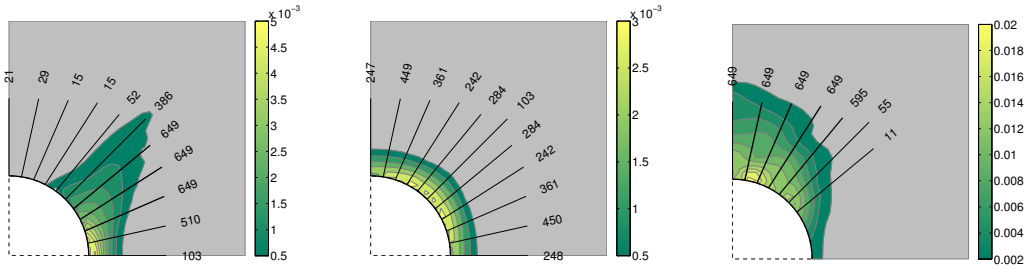

(a) (b) (c)

(a) (b) (c)

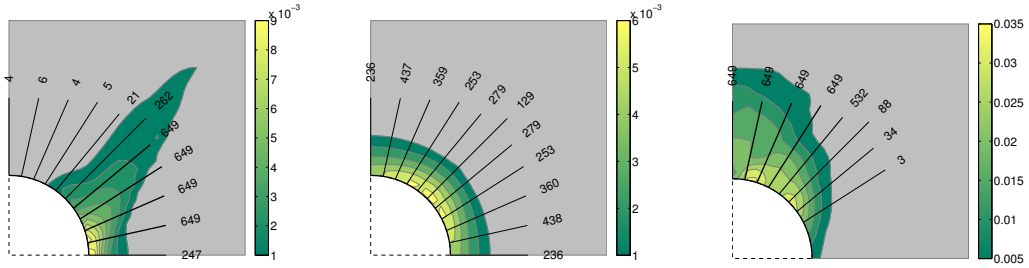

(d) (e) (f)

(d) (e) (f)

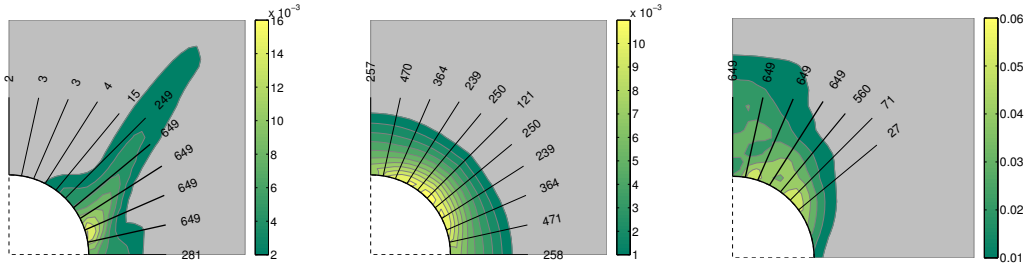

(g) (h) (i)

(g) (h) (i)

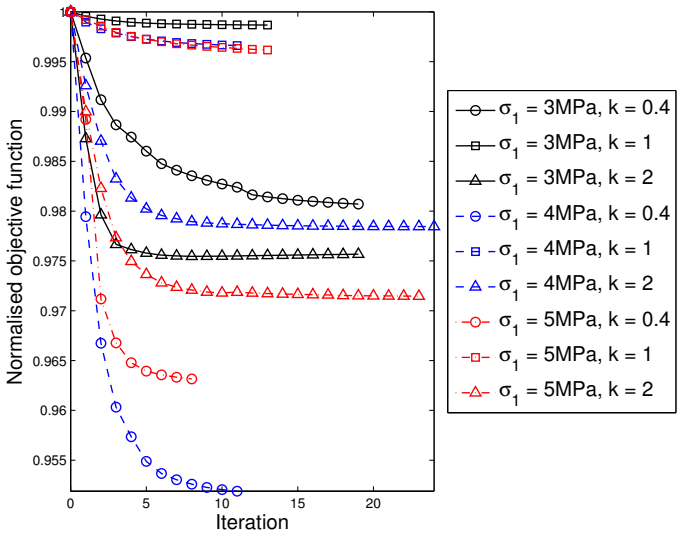

(j)

(j)

FIG. 7

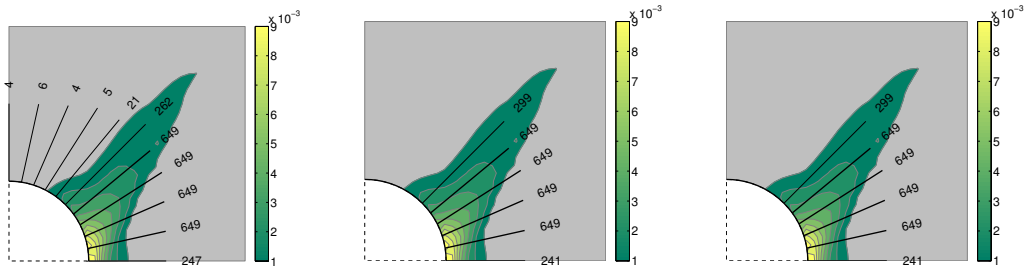

(a) (b) (c)

(a) (b) (c)

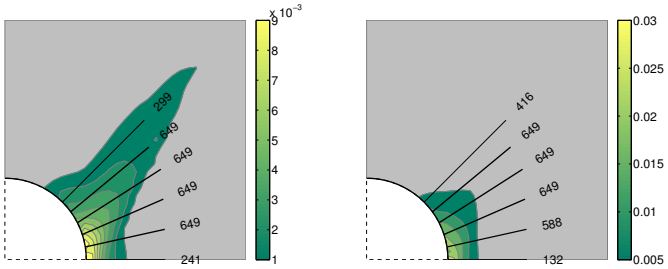

(d) (e)

(d) (e)

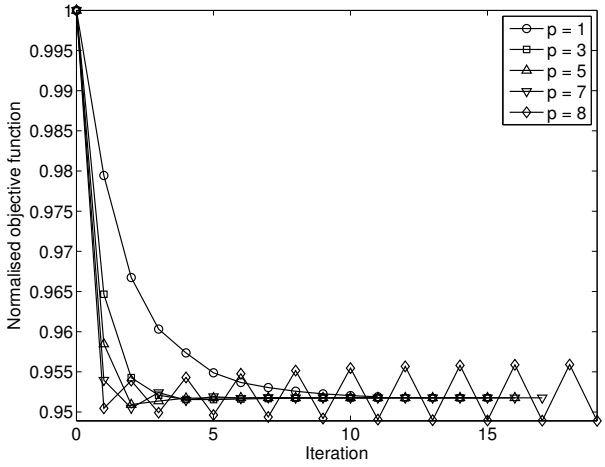

(f)

(f)

FIG. 8

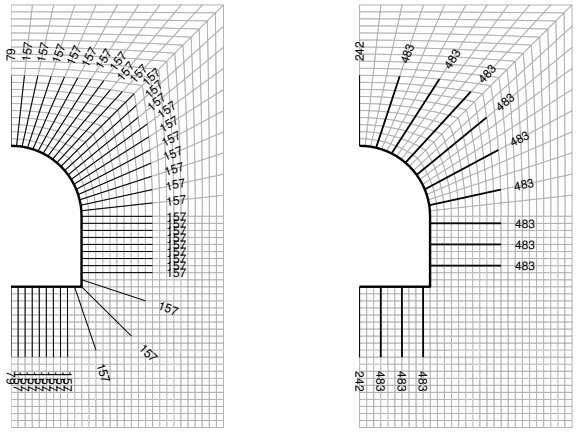

(a) (b)

(a) (b)

FIG. 9

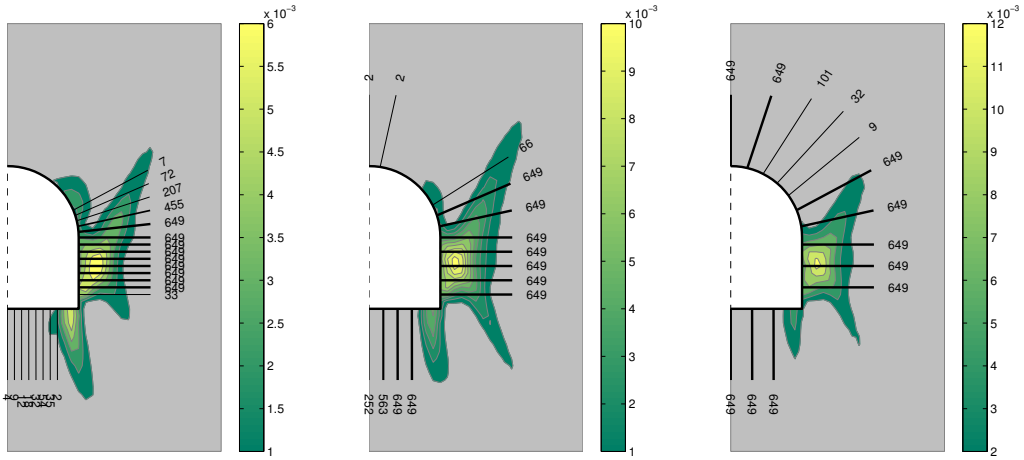

(a) (b) (c)

(a) (b) (c)

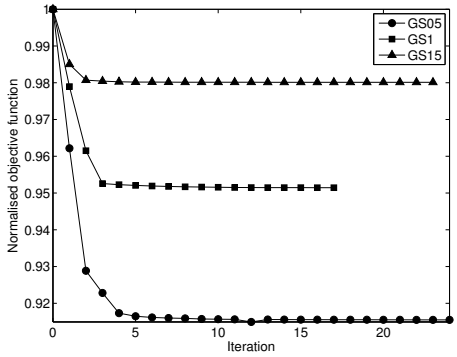

(d)

(d)

FIG. 10

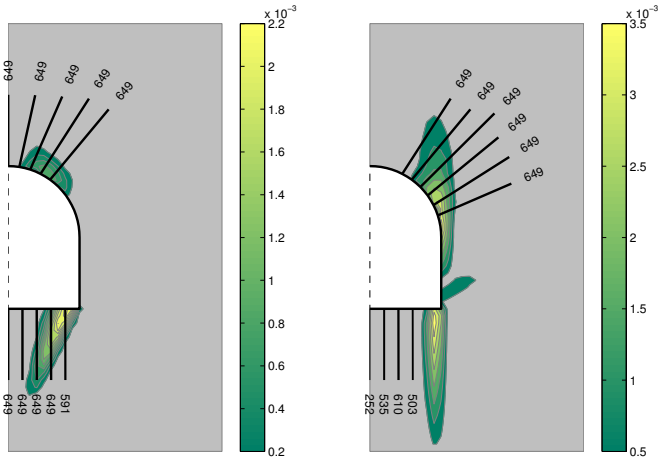

(a) (b)

(a) (b)

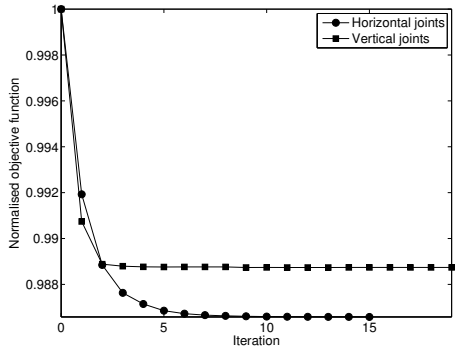

(c)

(c)

FIG. 11

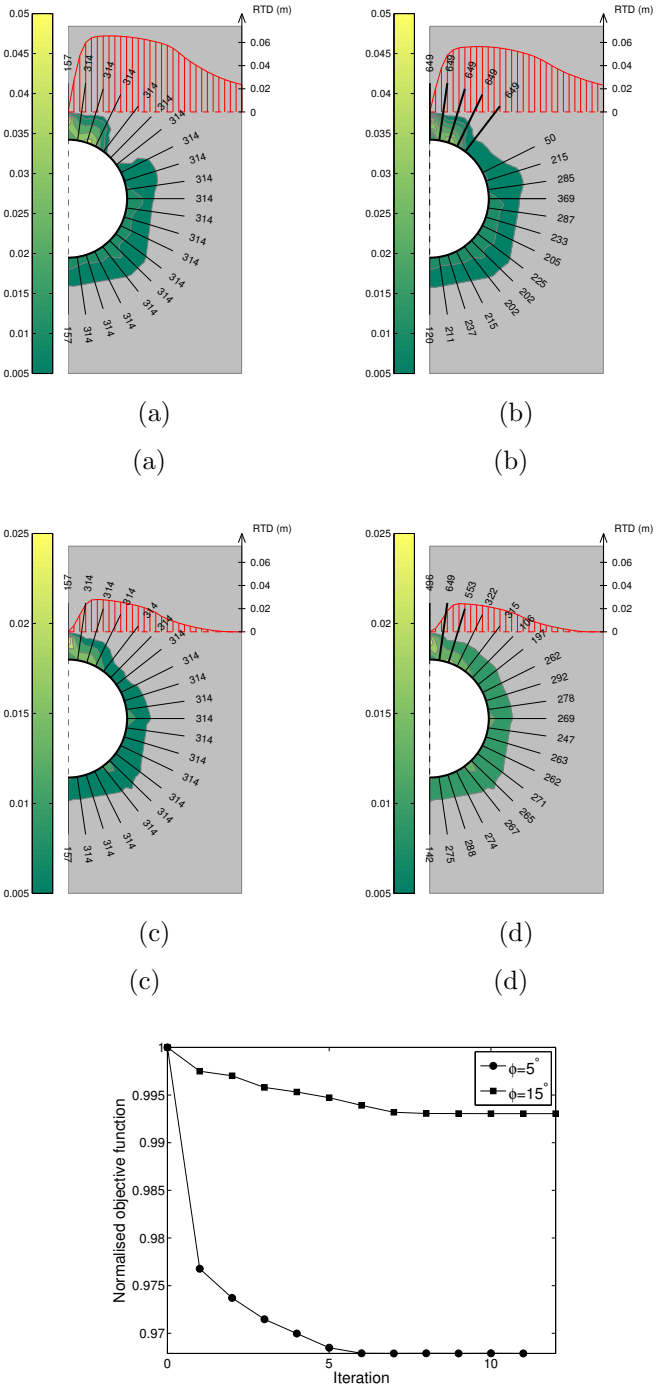

(a) (b)

(a) (b)

(c) (d)

(c) (d)

(e)

(e)

FIG. 12